# Modification of Laminar Flow Ultrafine Condensation Particle Counters for the Enhanced Detection of 1 nm Condensation Nuclei

**Chongai Kuang,[1] Modi Chen,[2] Peter H. McMurry,[2] and Jian Wang[1]**

[1]*Atmospheric Sciences Division, Brookhaven National Laboratory, Upton, New York, USA*
[2]*Department of Mechanical Engineering, University of Minnesota, Minneapolis, Minnesota, USA*

This paper describes simple modifications to thermally diffusive laminar flow ultrafine condensation particle counters (UCPCs) that allow detection of ∼1 nm condensation nuclei with much higher efficiencies than have been previously reported. These non-destructive modifications were applied to a commercial butanol-based UCPC (TSI 3025A) and to a diethylene glycol-based UCPC (UMN DEG-UCPC). Size and charge dependent detection efficiencies using the modified UCPCs (BNL 3025A and BNL DEG-UCPC) were measured with high resolution mobility classified aerosols composed of NaCl, W, molecular ion standards of tetra-alkyl ammonium bromide, and neutralizer-generated ions. With negatively charged NaCl aerosol, the BNL 3025A and BNL DEG-UCPC achieved detection efficiencies of 37% (90× increase over TSI 3025A) at 1.68 nm mobility diameter (1.39 nm geometric diameter) and 23% (8× increase over UMN DEG-UCPC) at 1.19 nm mobility diameter (0.89 nm geometric diameter), respectively. Operating conditions for both UCPCs were identified that allowed negatively charged NaCl and W particles, but not negative ions of exactly the same mobility size, to be efficiently detected. This serendipitous material dependence, which is not fundamentally understood, suggests that vapor condensation might sometimes allow for the discrimination between air "ions" and charged "particles." As a detector in a scanning mobility particle spectrometer (SMPS), a UCPC with this strong material dependence would allow for more accurate measurements of sub-2 nm aerosol size distributions due to the reduced interference from neutralizer-generated ions and atmospheric ions, and provide increased sensitivity for the determination of nucleation rates and initial particle growth rates.

## INTRODUCTION

Direct measurements of aerosol nucleation from gaseous precursors are of fundamental and practical interest in the study of gas-to-particle conversion, and play an important role in diverse fields including nanomaterials synthesis, nanoparticle health effects, and atmospheric new particle formation. Butanol-based ultrafine condensation particle counters (UCPCs) have traditionally been used to detect nanoparticles with diameters down to 3 nm (Stolzenburg and McMurry 1991). However, measurements of nanoparticles smaller than this are needed to directly obtain nucleation rates and to better understand nucleation mechanisms. Recent advances in UCPC development have enabled mobility-classified aerosol detection in the sub-2 nm mobility diameter range in the laboratory (Iida et al. 2009; Sipilä et al. 2009) and in the atmosphere (Jiang et al. 2011a), typically through the use of a low vapor pressure, high surface tension working fluid such as diethylene glycol (Iida et al. 2009) or by operating the UCPC with homogeneous nucleation of the working fluid (Mordas et al. 2008; Sipilä et al. 2009). In this study, a commercial butanol-based UCPC (TSI 3025A [Stolzenburg and McMurry 1991]) and a diethylene glycol-based UCPC developed at the University of Minnesota (UMN DEG-UCPC [Iida et al. 2009]) were modified non-destructively to increase particle detection efficiency down to 1 nm mobility diameter while eliminating interference from homogeneous nucleation of the working fluid. The size-dependent detection efficiencies of the modified UCPCs, hereafter referred to as the BNL 3025A and the BNL DEG-UCPC, were then characterized with challenge aerosols of different composition and polarity.

## EXPERIMENT

### Instrument Description

The BNL 3025A and BNL DEG-UCPC are laminar flow, thermally diffusive ultrafine CPCs based on the designs of the TSI 3025A UCPC (Stolzenburg and McMurry 1991) and of the UMN DEG-UCPC (Iida et al. 2009; Jiang et al. 2011a), respectively. The BNL 3025A was reversibly modified from a
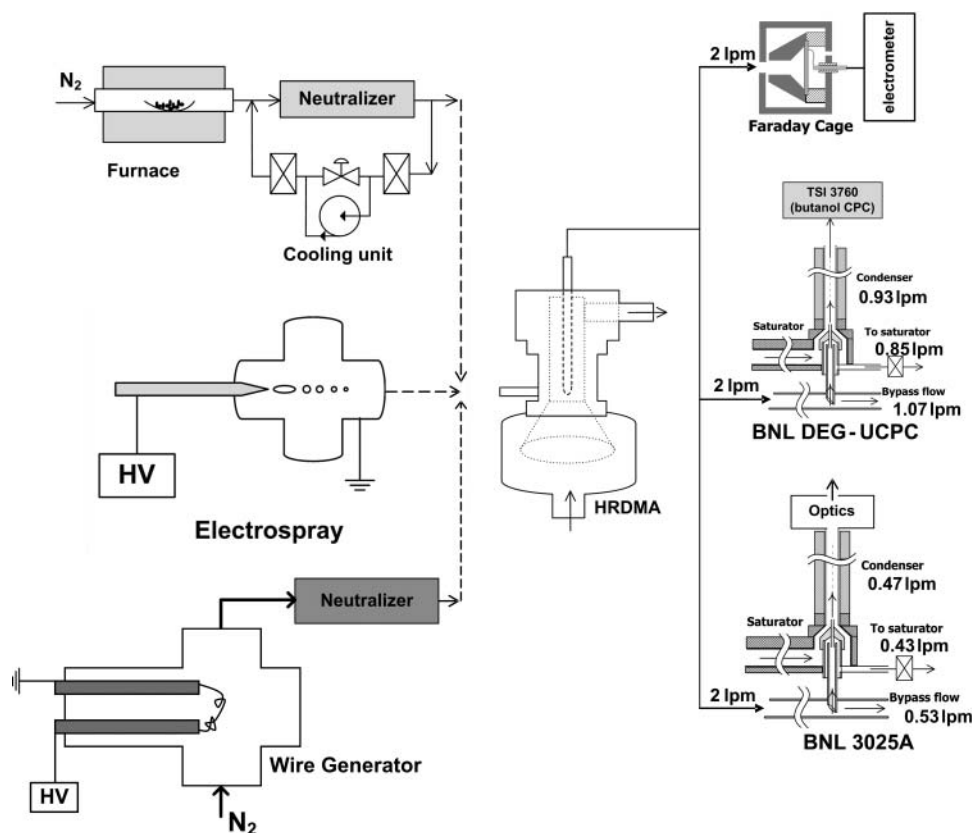
FIG. 1. Experimental setup for UCPC characterization, adapted from Jiang et al. (2011a).

commercial TSI 3025A by: (1) increasing the saturator ($T_s$) and optics ($T_o$) temperatures, from the standard operating set-points of 37 and 39°C, to 44 and 46°C, respectively, and by (2) increasing the condenser flow-rate ($Q_c$) from the standard operating set-point of 0.30 to 0.47 lpm. The BNL DEG-UCPC consists of a TSI 3025A with the laser detection unit removed (an "activation" unit), followed by a butanol-based TSI 3760 CPC (Wiedensohler et al. 1997) as the downstream "booster" to continue growth of DEG droplets to an optically detectable size, since the size of DEG droplets exiting the "activation" unit are smaller than 1 $\mu$m (Iida et al. 2009). The "activation" unit is connected to the "booster" with a length of 25 cm tubing at room temperature (25°C). The BNL DEG-UCPC was reversibly modified relative to the UMN DEG-UCPC by: (1) increasing $T_s$ from 59 to 70°C, and (2) increasing $Q_c$ from 0.30 to 0.93 lpm. Aerosol flow-rates through the sample capillary ($Q_a$) for both instruments were maintained at approximately 9% of their respective condenser flow-rates. Temperature modifications for both UCPCs were accomplished through the instrument serial command interface.

### Instrument Modification

For each UCPC, $T_s$ and $Q_c$ were increased from their nominal operating set-points so as to increase the instrument saturation ratio while minimizing the detection of droplets formed through homogeneous nucleation of the working fluid, respec-

tively. In these experiments, each UCPC was sampling room air through an absolute HEPA filter so as to measure the rate of working fluid droplet detection. For the BNL 3025A, $T_s$ was first increased to 44°C while $T_c$ and $Q_c$ were held fixed at 10°C and 0.30 lpm, respectively, so as to match the instrument operating conditions of the butanol-based pulse height analysis (PHA) UCPC (Sipilä et al. 2009). $T_o$ was set to 46°C to prevent butanol condensation in the optics block. $Q_c$ was then varied by adjusting the operating set-point of the internal pump through the instrument onboard calibration protocol (TSI 2002). The stable operating condition was then found by adjusting $Q_c$ until the detection rate of droplets, formed from the homogeneous nucleation of the working fluid within the condenser, was less than 1 particle count over a sampling interval of 5 min, a maximum noise criterion based on a typical measurement time interval for a scanning mobility particle spectrometer (SMPS) (Iida et al. 2009). For the BNL DEG-UCPC, the stable operating condition was found using a similar method. The modified UCPCs were then characterized using these modified operating parameters.

### Instrument Characterization

The experimental schematic for determining the size, charge, and composition dependent particle detection efficiencies of the two UCPCs is based on that of Jiang et al. (2011a) and illustrated in Figure 1. Four different methods for producing challenge

aerosols were used in this study: (1) electrospray generation of molecular ion mobility standards (tetra-heptyl and tetra-dodecyl ammonium bromide ions) (Ude and De la Mora 2005), (2) evaporation of solid sodium chloride (NaCl) in a tube furnace followed by rapid vapor condensation (Scheibel 1983), (3) tungsten (W) aerosol formation using a wire generator (Peineke et al. 2006), and (4) neutralizer ion generation through radioactive decay. $N_2$ was used as a carrier gas in each aerosol generation method. All challenge aerosols were then mobility classified with a high resolution differential mobility analyzer (HRDMA) (Herrmann et al. 2000), producing monodisperse molecular ion mobility standards, pseudo-monodisperse NaCl and W aerosols, and pseudo-monodisperse neutralizer ion aerosols according to the HRDMA operating conditions of Jiang et al. (2011a). The HRDMA sheath inlet flow was filtered with two absolute HEPA filters, resulting in sheath particle concentrations that were smaller than 0.1 $cm^{-3}$ for the majority of measurements. The tetra-heptyl ammonium bromide (THABr) ions have a mobility equivalent diameter of 1.47 and 1.78 nm for the monomer and the dimer, respectively, while the tetra-dodecyl ammonium bromide (TDDABr) ions have a mobility equivalent diameter of 1.70 nm for the monomer (Ude and De la Mora 2005). Corresponding geometric diameters for these 3 molecular ion species are estimated to be 1.17 nm (THABr monomer), 1.48 nm (THABr dimer), and 1.40 nm (TDDABr monomer) according to the methods of Ku and de la Mora (2009) and Larriba et al. (2011). Detection efficiencies for positive and negative ions generated inside the Po-210 neutralizer were measured by placing an absolute filter upstream of the neutralizer. Tubing lengths and sample flow-rates between the exit of the HRDMA and the inlet of each UCPC and the aerosol electrometer were identical so as to maintain the same particle diffusion losses along those tubing lengths. The UCPC detection efficiency at a given particle size was determined from the ratio of the particle concentration measured by the UCPC (or the TSI 3760 in the case of the BNL DEG-UCPC) to that measured by an aerosol electrometer (Liu and Pui 1974). Detection efficiency results will be subsequently presented as percent detection efficiencies.

## RESULTS AND DISCUSSION

### Modification of Instrument Operating Conditions

The results of the UCPC operating condition modification experiments are shown in Figure 2, where the detection rate of droplets formed by homogeneous nucleation of the working fluid was found to decrease sharply with increasing $Q_c$ for both instruments. For the BNL 3025A and the BNL DEG-UCPC, the maximum noise criterion for stable operation (1 particle count or less over 5 min when sampling filtered air) was achieved at condenser flow-rates of 0.47 and 0.80 lpm, respectively. For the subsequent UCPC characterization experiments, the following operating parameters were chosen to both enhance the detection efficiency and meet the noise criterion: (1) $T_c/T_s/T_o = 10°C/44°C/46°C$ and $Q_a/Q_c = 0.043$ lpm/0.47 lpm for the BNL
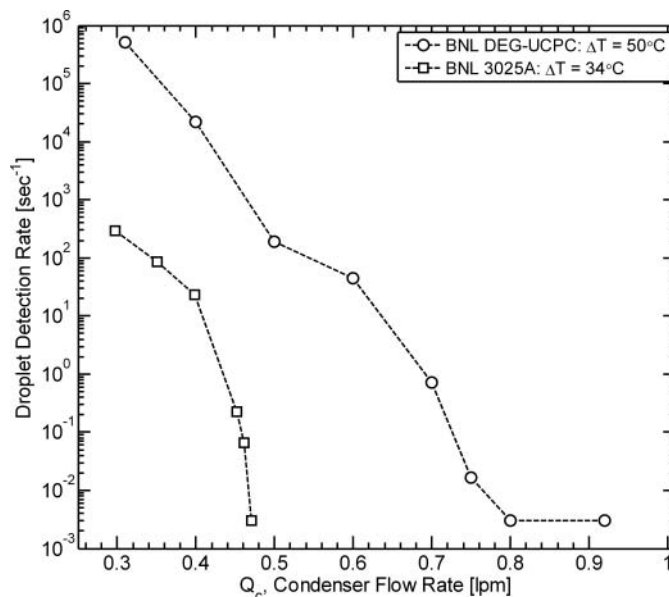


FIG. 2. Detection rate of particles formed by homogeneous nucleation of the working fluid as a function of condenser flow-rate ($Q_c$) for the BNL DEG-UCPC and BNL 3025A at the saturator ($T_s$)/condenser ($T_c$) temperature differences $\Delta T$ ($\Delta T = T_s - T_c$) shown in the legend. A homogeneous nucleation rate of 0.003 $sec^{-1}$ corresponds to a measurement of 1 particle count or less over the measurement time interval (5 min). Modified $Q_c$ values of 0.47 and 0.93 lpm were chosen for stable operation of the BNL 3025A and BNL DEG-UCPC, respectively.

3025A, and (2) $T_c/T_s = 20°C/70°C$ and $Q_a/Q_c = 0.083$ lpm/0.93 lpm for the BNL DEG-UCPC. During the characterization experiments, values for $Q_a$ and $Q_c$ were within 2% of their respective set-points for both instruments. For the BNL 3025A, values of $T_c$, $T_s$, and $T_o$ were within 0.1°C of their respective set-points, and for the BNL DEG-UCPC, values of $T_c$ and $T_s$ were within 0.2 and 0.1°C of their respective set-points.

A possible explanation for this decrease in the detection rate of homogeneously nucleated droplets with increasing condenser flow-rate is that increasing $Q_c$ leads to a reduction in residence time within the condenser, thus, a homogeneously nucleated droplet of working fluid would have less time to grow to a detectable size before exiting the condenser and being counted. For the BNL 3025A, this threshold size corresponds to the minimum detectable size of the optics, estimated to be several micrometers in diameter (TSI 2002), and for the BNL DEG-UCPC, this threshold size is ∼10 nm, the minimum detectable size of the TSI 3760 "booster" (Wiedensohler et al. 1997). The theoretical relationship between condenser flow-rate and homogeneously nucleated droplet diameter was investigated for the case of the BNL 3025A by numerically modeling the condenser saturation ratio profile using COMSOL Multiphysics (a finite element analysis software package), assuming: (1) a condenser geometry identical to that of a TSI 3025A (Stolzenburg and McMurry 1991), (2) $T_c/T_s = 10°C/44°C$, and (3) laminar flow with negligible butanol vapor depletion due to droplet growth. Modeled
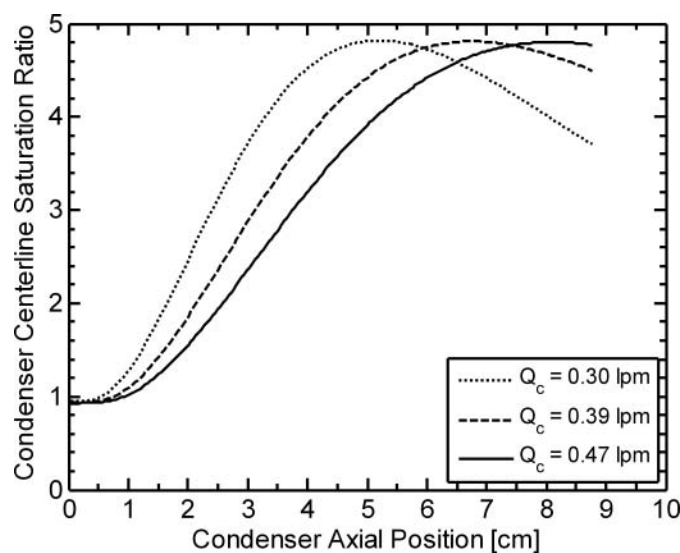
FIG. 3.    Modeled centerline profiles of the butanol saturation ratio as a function of axial position within the condenser of the BNL 3025A ($T_c/T_s = 10°C/44°C$) at condenser flow-rates ($Q_c$) of 0.30 (normal), 0.39, and 0.47 lpm (modified).



FIG. 4.    Model results for the diameter of an exiting butanol droplet as a function of condenser flow-rate ($Q_c$). Each point represents the modeled final diameter of a butanol droplet that forms at the peak in the centerline saturation ratio profile.

centerline saturation ratio profiles were generated for condenser flow-rates of 0.30 (normal), 0.39, and 0.47 lpm (modified), and shown in Figure 3 as a function of condenser axial position. The model results clearly show the shift in the peak of the centerline saturation ratio profile with increasing condenser flow rate; even at the modified condenser flow-rate of 0.47 lpm, the peak in the centerline saturation ratio profile is still within the condenser.

Using the modeled results for the condenser saturation ratio profile and the equations for droplet growth kinetics (Seinfeld and Pandis 2006), the diameter of a butanol droplet exiting the condenser (formed at the peak in the centerline saturation ratio profile) was modeled as a function of increasing condenser flow-rate, results of which are shown in Figure 4. As condenser flow-rate is increased, a droplet of butanol formed at the peak saturation ratio would have less time to grow before exiting the condenser and would consequently grow to a smaller final droplet diameter. At a high enough condenser flow-rate, homogeneously nucleated droplets would potentially not be detected at all. This dependence of final droplet diameter on condenser flow-rate is consistent with the results of Ahn and Liu (1990), who modeled droplet growth processes in an earlier model butanol-based CPC.

## Instrument Intercomparison

Intercomparisons of instrument performance between the UMN and BNL DEG-UCPCs and between the TSI and BNL 3025A UCPCs are presented in Figure 5, where size-dependent detection efficiencies for negative, singly-charged NaCl are presented for each UCPC. The relative uncertainty for each measurement of detection efficiency is less than 10%. The overall relative uncertainty was determined by propagating the uncer-
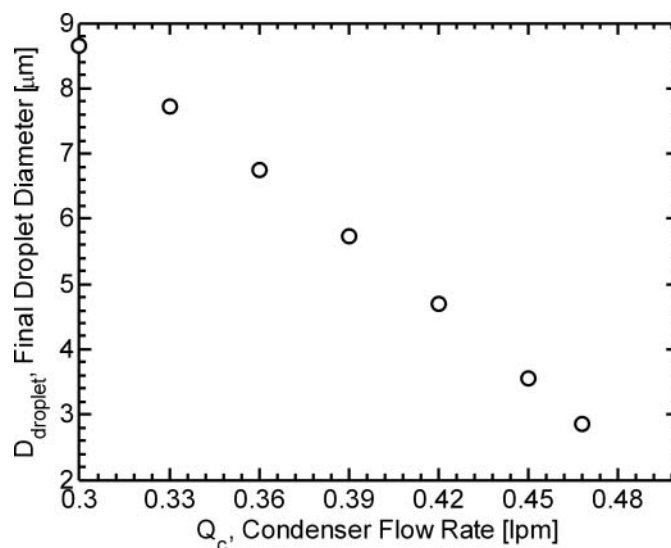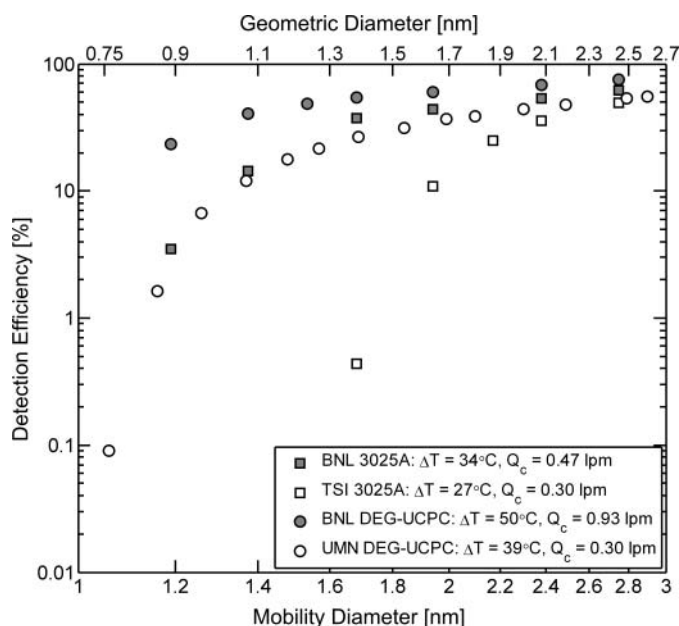


FIG. 5.    Intercomparisons of detection efficiencies for negative, singly charged NaCl particles as a function of mobility diameter between modified UCPCs (BNL 3025A and BNL DEG-UCPC) and their unmodified counterparts (TSI 3025A and UMN DEG-UCPC). Values for the corresponding geometric diameter are shown on the upper abscissa, estimated according to Larriba et al. (2011). Also listed for each UCPC are the operating values of the saturator ($T_s$)/condenser ($T_c$) temperature difference $\Delta T$ ($\Delta T = T_s - T_c$) and condenser flow-rate ($Q_c$) that yield enhanced performance. The corresponding modified aerosol flow-rate ($Q_a$) is 0.043 lpm for the BNL 3025A and 0.083 lpm for the BNL DEG-UCPC. The relative uncertainty for each measurement of detection efficiency is less than 10%.

tainty in the UCPC concentration measurement (derived from the statistical error associated with particle counting) and the uncertainty in the aerosol electrometer concentration measurement (derived from the variance of the electrometer signal) over the measurement time interval of 30 s. The BNL 3025A displays a significant improvement in performance compared to the TSI 3025A, where increasing $T_s$ and $Q_c$ have increased the detection efficiency of 1.68 nm mobility diameter particles by nearly two orders of magnitude from 0.4 to 37%, while eliminating interference from homogeneous nucleation of the working fluid. This increase in detection efficiency is due in part to the increase in the penetration efficiency of 1.68 nm mobility diameter particles through the sample capillary (where the majority of particle diffusional losses occur), which was estimated according to Stolzenburg and McMurry (1991) and was found to increase by a factor of 1.2 as the sample capillary flow-rate ($Q_a$) was increased from 0.030 (normal) to 0.043 lpm (modified). Existing butanol-based CPCs that detect sub-2 nm particles can only do so with significant homogeneous nucleation of the working fluid (Mordas et al. 2008; Sipilä et al. 2009), precluding their use as particle detectors in a SMPS. This simple, non-destructive modification to the TSI 3025A presents a straightforward method of extending the lower size detection limit while meeting the noise criterion for use as a detector in a SMPS system. The BNL DEG-UCPC also displays an enhanced performance compared to the UMN DEG-UCPC, where the detection efficiency of 1.19 nm mobility diameter particles has been increased to 23%, a nearly 8× improvement over the UMN DEG-UCPC detection efficiency at the same size. Part of this enhanced detection is due to the increased penetration efficiency of 1.19 nm mobility diameter particles through the sample capillary, which was estimated to increase by a factor of 2 as the sample capillary flow-rate ($Q_a$) was increased from 0.030 (normal) to 0.083 lpm (modified).

## BNL 3025A

A composite of the BNL 3025A instrument performance is presented in Figure 6, where size-dependent detection efficiencies for the negatively and positively charged challenge aerosols are shown. Due to the overlap in mobility between charged particles and neutralizer-generated ions below 1.5 nm mobility diameter, the actual detection efficiencies for positively and negatively charged NaCl and W aerosol in that size range are likely to be higher compared to the reported detection efficiencies (Iida et al. 2009). This underestimation is due to the fact that the aerosol electrometer detects all of the incoming charged nuclei (ions and particles) while the BNL 3025A detects only a small fraction of neutralizer-generated ions. Relative uncertainties for the reported detection efficiencies are less than 10%, except for the negative neutralizer ions (∼50% relative uncertainty). As seen in Figure 6, there is a strong dependence of detection efficiency on particle composition and polarity below about 2.2 nm mobility diameter. For negatively charged aerosol, nanoparticles composed of NaCl are preferentially detected compared to
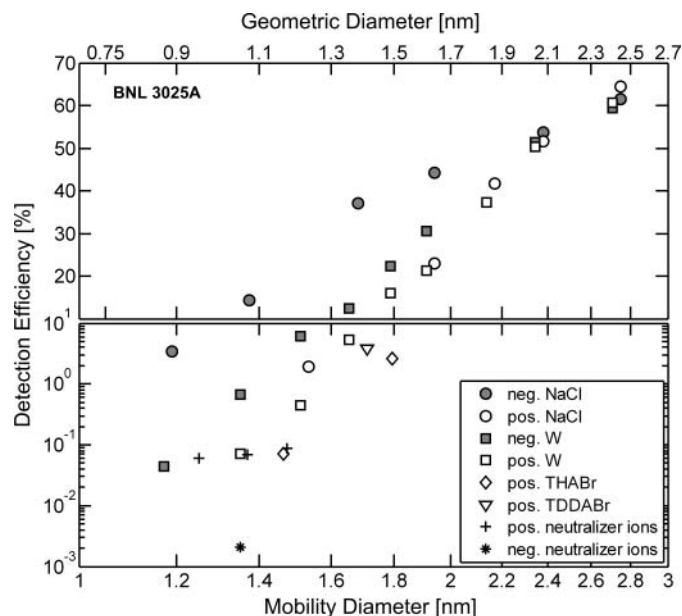


FIG. 6. A composite of the BNL 3025A detection efficiencies for the listed aerosol compositions and polarities as a function of mobility diameter. Values for the corresponding geometric diameter are shown on the upper abscissa, estimated according to Larriba et al. (2011). Note, the ordinate scale is linear above 10% and is logarithmic below 10%. The relative uncertainty for each measurement of detection efficiency is less than 10%, except for the negative neutralizer ions (relative uncertainty ∼50%). Results were obtained with the following modified UCPC operating parameter values: $T_c/T_s/T_o = 10°C/44°C/46°C$, and $Q_a/Q_c = 0.043$ lpm/0.47 lpm.

those composed of W. For positively charged aerosol, nanoparticles composed of NaCl and W are preferentially detected compared to the positively charged molecular ions and neutralizer-generated ions. While this composition dependence is qualitatively consistent with that obtained with the butanol-based PHA-UCPC (Sipilä et al. 2009), there is one quantitative difference between the two UCPCs that is worth highlighting: while the detection efficiencies of positively charged particles were similar between the BNL 3025A and the PHA-UCPC (around 15% for 1.78 nm mobility diameter W and WO$_x$ particles, respectively), the detection efficiencies for positive neutralizer-generated ions with the BNL 3025A (0.06–0.08%) were around 80× lower than detection efficiencies of similarly sized positive neutralizer-generated ions obtained with the PHA-UCPC. Detection efficiencies for the THABr monomer and dimer obtained with the BNL 3025A (0.07–2.6%) were also lower than those obtained with the PHA-UCPC by at least 10×.

This strong detection discrimination between particles and ions at a given polarity helps to minimize the potential interference from neutralizer-generated ions that arises whenever sub-2 nm aerosol size distribution measurements are made using an SMPS (Iida et al. 2009; Jiang et al. 2011a). The low detection efficiency of neutralizer-generated ions suggests that atmospheric ions would also likely be detected with a low efficiency, which is a distinct advantage over an electrometer-based ion

mobility spectrometer such as the NAIS (Kulmala et al. 2007), which does not distinguish between freshly nucleated particles and the atmospheric ions that are present throughout the day (Jiang et al. 2011b). The enhanced detection of sub-2 nm nuclei combined with the strong detection discrimination between charged particles and ions makes the BNL 3025A a suitable detector for an SMPS system designed for acquiring size distributions down to 1 nm.

For a given particle composition and size, negatively charged particles were preferentially detected compared to positively charged particles, while positive neutralizer-generated ions were preferentially detected ($\sim$0.05% detection efficiency) compared to negative neutralizer-generated ions ($\sim$0.002% detection efficiency). This particle detection charge preference of negative over positive has been observed in a number of experimental studies using different particle compositions, working fluids, and CPC designs (Winkler et al. 2008; Iida et al. 2009; Sipilä et al. 2009), while the reversal in charge preference for neutralizer-generated ions (positive over negative) has been observed in the studies of Sipilä et al. (2009) and Vanhanen et al. (2011).

## BNL DEG-UCPC

A composite of the BNL DEG-UCPC instrument performance is depicted in Figure 7, where size-dependent detection efficiencies for the negatively and positively charged challenge aerosols are shown. Relative uncertainties for the reported detection efficiencies are less than 10%. As seen in Figure 7, there is a strong dependence of detection efficiency on particle composition and polarity below about 1.8 nm mobility diameter, following the same qualitative trends as with the BNL 3025A. Generally, the detection efficiencies for the NaCl and W challenge aerosols were higher than those acquired with the BNL 3025A. Interestingly, however, there was no statistically significant detection of either negative or positive neutralizer-generated ions, and the detection efficiencies of the molecular ion mobility standards (THABr and TDDABr) were also lower compared to those acquired with the BNL 3025A, ranging 0.005–0.5%. Due to the overlap in mobility between charged particles and neutralizer-generated ions below 1.5 nm mobility diameter, combined with the observation that the BNL DEG-UCPC detects virtually none of the neutralizer-generated ions while the aerosol electrometer detects all charged nuclei, the actual detection efficiencies of NaCl and W nanoparticles below 1.5 nm mobility diameter are likely to be higher than the reported detection efficiencies. Due to the high detection efficiency of $\sim$1 nm nuclei and the zero detection of neutralizer-generated ions, the BNL DEG-UCPC would be an ideal detector in an SMPS system designed to acquire size distributions down to 1 nm. The fact that detection efficiencies of particles (NaCl and W) increased while those of ions (charger-generated and molecular ion standards) decreased when switching working fluids from butanol to DEG is unexpected and bears no clear explanation. This result suggests that the different ways in which the working fluid interacts with par-
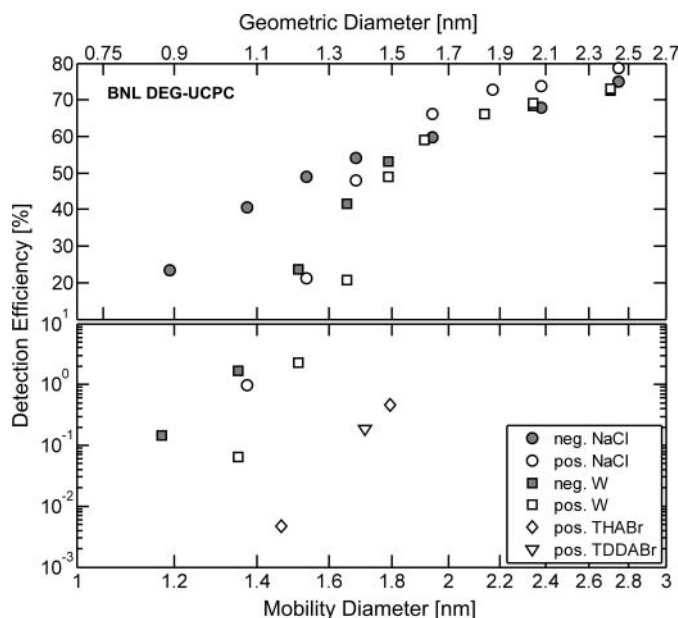


FIG. 7. A composite of the BNL DEG-UCPC detection efficiencies for the listed aerosol compositions and polarities as a function of mobility diameter. Values for the corresponding geometric diameter are shown on the upper abscissa, estimated according to Larriba et al. (2011). Note, the ordinate scale is linear above 10% and is logarithmic below 10%. The relative uncertainty for each measurement of detection efficiency is less than 10%. Results were obtained with the following modified UCPC operating parameter values: $T_c/T_s$ = 20°C/70°C, and $Q_a/Q_c$ = 0.083 lpm/0.93 lpm.

ticles and ions is itself a function of working fluid. Further work is needed to understand this result.

## CONCLUSIONS

In this study, a non-destructive method for increasing the detection efficiencies of thermally diffusive laminar flow UCPCs has been developed and applied to a butanol-based UCPC (BNL 3025A) and a diethylene glycol-based UCPC (BNL DEG-UCPC). By increasing both the instrument operating temperatures and the condenser flow-rates, the detection efficiencies at the smallest detectable sizes were substantially increased while at the same time eliminating interference from homogeneous nucleation of the working fluid. Using negatively charged NaCl, the BNL 3025A detected 1.68 nm mobility diameter particles (1.39 nm geometric diameter) with an efficiency of 37% (90× improvement over TSI 3025A) while the BNL DEG-UCPC detected 1.19 nm mobility diameter particles (0.89 nm geometric diameter) with an efficiency of 23% (8× improvement over the UMN DEG-UCPC). Detection efficiencies of neutralizer-generated ions were very low (<1% for the BNL 3025A and 0% for the BNL DEG-UCPC). The high particle detection efficiencies at sizes down to 1 nm geometric diameter, combined with the strong detection discrimination between particles and ions and the elimination of counting noise from homogeneous nucleation, makes both the BNL 3025A and the BNL

DEG-UCPC ideal detectors in a 1 nm SMPS system. The detection efficiency of atmospheric ions is likely to be very low as well, further reducing the interference from species that do not participate in new particle formation, for instance.

## REFERENCES

Ahn, K. H., and Liu, B. Y. H. (1990). Particle Activation and Droplet Growth Processes in Condensation Nucleus Counter I. Theoretical Background. *J. Aerosol Sci.* 21:249–261.

Herrmann, W., Eichler, T., Bernardo, N., and Fernández de la Mora, J. (2000). *Turbulent Transition Arises at Reynolds Number 35,000 in a Short Vienna Type Dma with a Large Laminarization Inlet*. AAAR, St. Louis, MO.

Iida, K., Stolzenburg, M. R., and McMurry, P. H. (2009). Effect of Working Fluid on Sub-2 nm Particle Detection with a Laminar Flow Ultrafine Condensation Particle Counter. *Aerosol Sci. Technol.* 43:81–96.

Jiang, J., Chen, M., Kuang, C., Attoui, M., and McMurry, P. H. (2011a). Electrical Mobility Spectrometer Using a Diethylene Glycol Condensation Particle Counter for Measurement of Aerosol Size Distributions Down to 1 nm. *Aerosol Sci. Technol.* 45:510–521.

Jiang, J., Zhao, J., Chen, M., Eisele, F. L., Scheckman, J., Williams, B. J., Kuang, C., and McMurry, P. H. (2011b). First Measurements of Neutral Atmospheric Cluster and 1-2 nm Particle Number Size Distributions During Nucleation Events. *Aerosol Sci. Technol.* 45:2–5.

Ku, B. K., and de la Mora, J. F. (2009). Relation between Electrical Mobility, Mass, and Size for Nanodrops 1–6.5 nm in Diameter in Air. *Aerosol Sci. Technol.* 43:241–249.

Kulmala, M., Riipinen, I., Sipilä, M., Manninen, H. E., Petäjä, T., T., Junninen, H., Maso, M. D., Mordas, G., Mirme, A., and Vana, M. (2007). Toward Direct Measurement of Atmospheric Nucleation. *Science* 318:89.

Larriba, C., Hogan, C. J., Attoui, M., Borrajo, R., Garcia, J. F., and de la Mora, J. F. (2011). The Mobility–Volume Relationship Below 3.0 Nm Examined by Tandem Mobility–Mass Measurement. *Aerosol Sci. Technol.* 45:453–467.

Liu, B. Y. H., and Pui, D. Y. H. (1974). A Submicron Aerosol Standard and the Primary, Absolute Calibration of the Condensation Nuclei Counter. *J. Colloid Interf. Sci.* 47:155–171.

Mordas, G., Sipila, M., and Kulmala, M. (2008). Nanometer Particle Detection by the Condensation Particle Counter UF-02proto. *Aerosol Sci. Technol.* 42:521–527.

Peineke, C., Attoui, M. B., and Schmidt-Ott, A. (2006). Using a Glowing Wire Generator for Production of Charged, Uniformly Sized Nanoparticles at High Concentrations. *J. Aerosol Sci.* 37:1651–1661.

Scheibel, H. G. (1983). Generation of Monodisperse Ag-and Nacl-Aerosols with Particle Diameters between 2 and 300 nm. *J. Aerosol Sci.* 14:113–126.

Seinfeld, J. H., and Pandis, S. N. (2006). *Atmospheric Chemistry and Physics: From Air Pollution to Climate Change*. John Wiley & Sons, New York.

Sipilä, M., Lehtipalo, K., Attoui, M., Neitola, K., Petäjä, T., Aalto, P. P., O'Dowd, C. D., and Kulmala, M. (2009). Laboratory Verification of PH-CPC's Ability to Monitor Atmospheric Sub-3 nm Clusters. *Aerosol Sci. Technol.* 43:126–135.

Stolzenburg, M. R., and McMurry, P. H. (1991). An Ultrafine Aerosol Condensation Nucleus Counter. *Aerosol Sci. Technol.* 14:48–65.

TSI. (2002). *Model 3025A Ultrafine Condensation Particle Counter Instruction Manual* (Revision I). TSI, Inc., St. Paul, MN.

Ude, S., and De la Mora, J. F. (2005). Molecular Monodisperse Mobility and Mass Standards from Electrosprays of Tetra-Alkyl Ammonium Halides. *J. Aerosol Sci.* 36:1224–1237.

Vanhanen, J., Mikkilä, J., Lehtipalo, K., Sipilä, M., Manninen, H. E., Siivola, E., Petäjä, T., and Kulmala, M. (2011). Particle Size Magnifier for Nano-CN Detection. *Aerosol Sci. Technol.* 45:533–542.

Wiedensohler, A., Orsini, D., Covert, D. S., Coffmann, D., Cantrell, W., Havlicek, M., Brechtel, F. J., Russell, L. M., Weber, R. J., and Gras, J. (1997). Intercomparison Study of the Size-Dependent Counting Efficiency of 26 Condensation Particle Counters. *Aerosol Sci. Technol.* 27:224–242.

Winkler, P. M., Steiner, G., Vrtala, A., Vehkamäki, H., Noppel, M., Lehtinen, K. E. J., Reischl, G. P., Wagner, P. E., and Kulmala, M. (2008). Heterogeneous Nucleation Experiments Bridging the Scale from Molecular Ion Clusters to Nanoparticles. *Science* 319:1374.